The Nature of [Ar III] Bright Knots in the Crab Nebula

Emily L. Schaller & Robert A. Fesen
6127 Wilder Laboratory, Department of Physics & Astronomy
Dartmouth College, Hanover, NH 03755

ABSTRACT

The kinematic and morphological properties of a string of [Ar III] bright knots in the Crab Nebula are examined using 1994 – 1999 *HST* WFPC-2 images of the remnant. We find that five southern [Ar III] bright knots exhibit ordinary radial motions away from the nebula's center of expansion with magnitudes consistent with their projected radial displacements. This result does not support the suggestion by MacAlpine et al. (1994) that these knots might be moving rapidly away from the Crab pulsar due to a collimated wind. The *HST* images also do not show that the [Ar III] knots have unusual morphologies relative to other features in the remnant. Our proper motion results, when combined with radial velocity estimates, suggest these knots have relatively low space velocities implying relatively interior remnant locations thus placing them closer to the ionizing radiation from the Crab's synchrotron nebula. This might lead to higher knot gas temperatures thereby explaining the knots' unusual line emission strengths as MacAlpine et al. (1994) suspected.

Subject headings: ISM: individual (Crab Nebula) - supernova remnants - ISM: kinematics and dynamics

1. Introduction

For over half a century, the Crab Nebula has played a key role as a laboratory for many seminal discoveries regarding supernovae and their remnants (Trimble 1985). It is also the brightest and best studied example of "plerionic" remnants which are powered by a compact central object (see reviews Kafatos & Henry 1985; Davidson & Fesen 1985).

Despite its many astronomical firsts, the detection by MacAlpine et al. (1994) of chains of semi-stellar, optical knots showing unusually strong [Ar III] line emission was both remarkable and puzzling. The discovery came about through a search looking for north-south, bi-polar axial phenomena directly associated with the Crab pulsar and related to the remnant's east-west band of strong helium emission filaments (Uomoto & MacAlpine 1987; MacAlpine et al. 1989; Fesen et al. 1992) and the N-S hourglass structure seen in polarized light of the Crab's synchrotron nebula (Michel et al. 1991).

Using a Fabry-Perot imager centered at 5015.3 Å, MacAlpine et al. (1994) found about a dozen, semi-stellar [O III] λ5007 emission knots aligned in arcs, perhaps helical (MacAlpine et al. 1992), from the pulsar's position with seven to the north and four to the south. The northern arc of knots appeared situated inside a corridor through the remnant's filamentary structure, the eastern edge of which seemed to merge with the western edge of the Crab's well-known northern "jet" (van den Bergh 1970). MacAlpine et al. (1994) suggested that this corridor containing the northern knots marked the presence of a directed, north-south collimated wind from the pulsar's vicinity and possibly associated with the pulsar's spin axis (MacAlpine et al. 1992).

Subsequent optical spectra of several of these knots revealed remarkably strong [Ar III] λ7136 and [S II] $\lambda\lambda$6716, 6731 line emission. The knots' strong [Ar III] line emission was deemed more remarkable than that of the [S II], leading MacAlpine et al. to refer them as "argo-knots". Their unusual [Ar III] line strength was interpreted as being due to either $N(Ar^{+2})/N(H^{+})$

ratios 5 − 10 higher than in typical Crab filaments, unusually high knot electron temperatures, or some process(es) not normally important in nebula astrophysics.

Perhaps most remarkable was the knots' apparent alignment with, and transverse velocities as high as 900 km s^{-1} away from, the Crab pulsar. The knots' arrangement in north and south arcs in striking alignment with the Crab pulsar was highly suggestive of a causal link. This is because the pulsar has a motion toward the northwest away from the Crab's expansion point of ≃125 km s^{-1} ($0''.011 \pm 0''.001$ yr^{-1}, PA = 290°; Wyckoff & Murray 1977). In addition to the location of the northern knots inside a filamentary corridor associated with the northern jet feature, MacAlpine et al. (1994) also found that the argo-knots' north-south alignment to be roughly perpendicular to an apparent east-west torus of high-helium filaments (Uomoto & MacAlpine 1987).

Positional measurements for the seven northern and four southern [Ar III] knots using ground-based images taken over a two year baseline (1991 – 1993) indicated proper motions of $\leq 0''.1$ yr^{-1} or ≤ 900 km s^{-1} at the Crab's 1830 pc distance (Davidson & Fesen 1985). Although their proper motion results had relatively large associated uncertainties ($\pm 0''.07$ yr^{-1}), MacAlpine et al. (1994) concluded that "All measured north or south motions are directed away from the pulsar, as expected".

This conclusion, when taken together with the knots' remarkable alignment with the pulsar's current position suggested a kinematic link between the pulsar and these so-called "argo-knots". However, if these knots were dynamically connected with a collimated wind off the pulsar, it would then mean that they comprise a small but previously unrecognized population of line emitting material within the remnant which does not participate in the remnant's radial expansion from the SN 1054 explosion point (Trimble 1968; Nugent 1998).

Non-radial motions in the Crab Nebula and in particular the presence of high-velocity, line-emitting gas moving rapidly away north and south from the pulsar is an unexpected discovery meriting further examination. In this paper, we present a proper motion and morphological study of a few of these knots using 1994-1999 *HST* WFPC-2 images of the Crab Nebula.

2. Observations

HST WFPC-2 images of the center of the Crab Nebula from 1994, 1995 and 1999 were obtained from the data archive at the Space Telescope Science Institute (Table 1). Figure 1 shows a 1995 *HST* WFPC2 image of the west-central region of the Crab Nebula taken with the [O III] λ5007 filter (F502N). The strong [Ar III] emitting knots N1 − N6 and S1 − S4 described by MacAlpine et al. 1994 are marked. Other nebular knots having similar "semi-stellar" [O III] morphologies are shown in the image and are labeled K1 − K9.

Because all 11 bright [Ar III] knots exhibit prominent [O III] λ5007 and [S II] λλ6716,6731 line emissions and positive radial velocities (+300 to +720 km s^{-1}; MacAlpine et al. 1994), WFPC-2 images taken using the [O III] F502N and [S II] F673N filters are well suited for studying these knots. Both filter bandpass centers are slightly redshifted (+360 km s^{-1}) and sufficiently wide (±800 km s^{-1}) to cover the knots' observed radial velocity range. In addition, the [O III] F502N image line center at 5013 Å is almost identical to the 5015 Å Fabry-Perot bandpass center used by MacAlpine et al. (1994) to measure the [Ar III] knots' kinematic properties.

Pairs of WFPC-2 1994 and 1999 images taken in [O III] and [S II] were each combined using the cosmic ray cleaning IRAF package "crrej". For the 1995 data, two pairs of images were available. These were also initially combined using "crrej" and then one pair was shifted and they were combined again using "crrej". The combined images for each year were then made into three mosaics representing 1994, 1995, and 1999, and rotated so that all were oriented with north up and east to the left.

Pixel image positions of four to six stars present on the 1994, 1995, and 1999 images were measured on each of the [O III] or [S II] WFPC-2 images ($0''.0996$ pixel^{-1}) using the IRAF task "imexamine". Image positions for the four southern [Ar III] bright nebular knots identified by (MacAlpine et al. 1994) were measured both by eye and by using "imexamine", with good agreement between the two methods. Since southern Knots S3 and S4 were not imaged on the 1994 images, their proper motion values were determined by comparing only the 1995 and 1999 images. Also measured was a similar but somewhat fainter, neighboring feature to Knots S1 and S2 which we call "S0" due to its smaller, projected distance from the pulsar than Knot S1. Pixel x and y offsets between the 1994/95 and 1999 images were then obtained and used to predict the 1999 pixel positions of the knots from the 1994 and 1995 images. Observed versus predicted knot positions divided by the time interval yielded α and δ (x and y) proper motion values.

Image pixel x and y differences for the reference stars were each averaged and the standard deviation of each was used as an estimate of the minimum measurement errors. These were added in quadrature with error estimates based on position differences between the [O III] and [S II] knots. Because of the large and irregular morphology of Knot S3, its proper motion determination is significantly more uncertain.

3. Results and Discussion

The Crab pulsar currently lies some $12'' - 13''$ northwest of the remnant's estimated expansion center (Trimble 1968; Nugent 1998). To determine whether, as MacAlpine et al. (1994) concluded, [Ar III] bright knots move away from the the Crab pulsar "as expected" due to a presumed collimated wind off the pulsar or instead move away the remnant's expansion center, we chose to examine the four southern [Ar III] bright knots they identified (S1–S4). We also included one additional likely [Ar III] knot (S0) we identified from the WFPC-2 [O III] images. This latter knot may be the one MacAlpine et al. (1994) referred to as being simply "to the south" of the pulsar.

Due to locations south*east* of the pulsar but south*west* of the Crab's center of expansion, the proper motions of the three innermost knots (S0, S1, & S2) would be expected to have either a strongly positive or negative right ascension term if moving away from the pulsar or the remnant's center of expansion respectively. That is, they ought to move toward the southeast if expanding away from the pulsar (PA $\leqslant 180°$) or toward the southwest if expanding away the Crab's expansion center (PA $\geqslant 180°$).

In contrast, all seven northern knots would be expected to show proper motions toward the northwest regardless of their origin point, thus making them a less powerful discrimination test without highly accurate positional measurements. In addition, the innermost northern knot, N1, lying just $4''$ north of the pulsar, is a poorly defined feature and lies projected against a relatively bright filamentary background making precise positional measurements more difficult.

3.1. Knot Proper Motions

Table 2 lists the positions of the five southern knots (relative to the central star just northeast of the pulsar; Star 16 of Wyckoff & Murray 1977), our proper motion measurements, and with those cited by MacAlpine et al. (1994). Within measurement uncertainites both data sets are in agreement. That is, although our estimated knot motions (except for Knot S1) are significantly smaller than those quoted by MacAlpine et al. (1994), they all lie within the MacAlpine et al.'s relatively large error bar of $\pm0\farcs07$ yr^{-1}.

However, it is puzzling why MacAlpine et al. (1994) concluded in favor of motions directed away from the pulsar with transverse velocities "of order" 900 km s^{-1} based on their poorly constrained proper motion measurements. Our east-west motions (δy values) of these five southern knots are more than an order of magnitude below the MacAlpine et al. (1994) detection limit. But they are in line with simple radial motion away from the center of expansion like that experienced by other remnant filamentary features. A comparison of our knot proper motion estimates relative to the projected displacements of the knots from the center of expansion determine by Trimble (1968) is given in Table 3. Here the average knot proper motions from the δx and δy displacements were calculated assuming these knots experienced the same acceleration as the general nebula leading to a derived explosion date $\simeq$ A.D. 1130 (Trimble 1968; Wyckoff & Murray 1977; Nugent 1998). As the table shows, our estimated knot proper motions are entirely consistent with the knots' projected radial displacements from the Crab's center of expansion. [Note the somewhat better agreement using the Nugent (1998) expansion center estimate.]

Table 3 also lists the implied transverse velocities for the knots based on our proper motion estimates, knot radial velocities reported by MacAlpine et al. (1994), and the resulting space velocities. The five knots' space velocities range from 440 and 740 km s^{-1}. This is on the low end of the remnant's $700 - 2200$ km s^{-1} filamentary expansion range (Davidson & Fesen 1985). This, in turn, places their location well inside the remnant's filamentary shell and thus relatively close to the X-ray and UV bright synchrotron nebula.

Our proper motion estimates for all five knots indicate motions away from the remnant's expansion center and not the pulsar. Specifically, the position angles (PA) for Knots S0–S2 are all $> 180°$, consistent with expected motions from either Trimble's or Nugent's estimated expansion centers. This is in contrast to the expected PA values of around 152° if these knots were moving away from the pulsar. Our results are graphically shown in Figure 2 where we plot the 100 yr proper motions of the five southern knots based on our measurements. As we found for the knots' total proper motion values, our measurements are in somewhat better agreement with the Nugent (1998) expansion center than that of Trimble (1968).

As a qualitative test of our results, we registered the 1994/95 images with the 1999 images and then blinked them. We found the [Ar III] knots' motions to be visually consistent with radial motion away from the center of expansion as opposed to away from the pulsar, supporting our quantitative results. We conclude the kinematics of these knots did not appear to be unusual relative to other nebular features.

We believe our derived knot proper motions to be more reliable than those of MacAlpine et al. (1994) for several reasons. First, they used ground-based [O III] images with a much coarser pixel scale ($0\farcs46$) compared the *HST* WFPC-2 images ($0\farcs1$) and with much lower image quality ($2''$ seeing vs. WFPC-2's FWHM of $0\farcs045$). Second, their images covered just a 2.0 yr time span compared to our 5.66 yr (1994–1999) and 4.81 yr (1995–1999) time coverage.

3.2. Knot Morphology

One criteria MacAlpine et al. (1994) used to help identify [Ar III] knots was a semi-stellar and/or isolated appearance on their ground-based images. When examined using the higher resolution WFPC-2 images, however, the knots described by MacAlpine et al. (1994) show a broad range of morphologies and angular dimensions. In Figure 3, we show enlargements of magnified WFPC-2 images for several of these [Ar III] knots. While many clearly do have a somewhat stellar appearance with diameters of $\simeq 0\farcs4 - 0\farcs7$, others appear fairly diffuse with diameters of up to $1\farcs5$ (e.g., Knots N1, N6 & S3).

Figure 3 also shows enlarged magnifications of nine other nebular knots (labeled K1 – K9) with sizes and morphologies similar to the "argoknots". One of these, K7, was noted by MacAlpine et al. (1994) as one of two other possible fainter and less distinct gas condensations. Similar knots are found throughout the central part of the remnant (see Fig. 1) and often lie near the north and south arcs of [Ar III] knots. The strong similarities in morphology of the [Ar III] knots to these other nebular knots, and the placement of these other knots around the N-S knot arc, suggests that the [Ar III] knots are not unusual remnant features.

4. Conclusions

Our study of the proper motions of five [Ar III] bright knots using *HST* WFPC2 data from 1994 to 1999 show ordinary radial motions away from the nebula's center of expansion with magnitudes consistent with their projected radial displacement. The measurements indicate the knots are moving away from the remnant's expansion center and not the pulsar. In addition, the [Ar III] knots do not appear to have unusual morphologies, and we have identified several other similarly appearing knots in the remnant. These results do not support the suggestion by MacAlpine et al. (1994) that these knots might be moving rapidly away from the Crab pulsar due to a collimated pulsar-driven wind or that these knots are unusual in appearance.

On the other hand, the spectral data of MacAlpine et al. (1994) clearly show they possess strong [O III] $\lambda\lambda$4959,5007 with unusually strong [Ar III] and [S II] line emissions. MacAlpine et al. and Lawrence et al. (1995) noted a possible spatial association of the northern argo-knots with a filament at a higher radial velocity (+900 to +1300 km s^{-1}). The [Ar III] bright knots were seen mainly at lower-intensity breaks in the filament's emission. They suggested that this might indicate that the material in the knots is derived from this filament possibly though some instability (Rayleigh-Taylor or Kelvin-Helmholtz).

Magnetic Rayleigh-Taylor instabilities at the interface of this filament and the pulsar-generated synchrotron nebula as discussed by Hester et al. (1996) and Sankrit et al. (1998) might well explain the [Ar III] knot morphologies. The tips of the Rayleigh-Taylor, finger-like filaments seen edge-on near the outer parts of the remnant (e.g., Filaments F, G, & H; Hester et al. 1996) show clumps of similar size and shape to the [Ar III] knots. The only difference here may be the viewing angle, where the [Ar III] knots are seen face-on.

The observed difference in radial velocity between the coincident filament and the chain of [Ar III] knot would be consistent with their more interior remnant positions. The estimated 440 – 740 km s^{-1} space velocities for these knots, at the extreme low end for the Crab's filaments, is also consistent with this picture. This would place them closer to the synchrotron nebula thus exposing them to higher X-ray and UV photoionization fluxes. This, in turn, might be the underlying cause for their strong [Ar III] line emission via higher gas temperatures as suspected by MacAlpine et al. (1994).

We thank V. Trimble for several helpful comments on the paper's presentation.

Table 1
WFPC-2 Images of the Crab Nebula

Date (U.T.)	Image ID	WFPC-2 Filter	Emission Line	Region Imaged	Exposures (s)
1994 Feb 23	U24R0203T–204T	F502N	[O III]	Center - NW	2000; 2000
1994 Mar 9	U24R0401T–402T	F673N	[S II]	Center - NW	2000; 2000
1995 Jan 2	U2BX0401T–402T	F673N	[S II]	Center - West	2000; 2300
1995 Jan 2	U2BX0403T–404T	F673N	[S II]	Center - West	2300; 2300
1995 Jan 5	U2BX0301T–302T	F502N	[O III]	Center - West	2000; 2300
1995 Jan 5	U2BX0303T–304T	F502N	[O III]	Center - West	2300; 2300
1999 Oct 24	U5D10305R–306R	F502N	[O III]	Center - SW	2600; 2600
1999 Oct 24	U5D10307R–308M	F673N	[S II]	Center - SW	1300; 1300

Table 2
[Ar III] Knot Proper Motions

	1995.0[a]		This paper			MacAlpine et al.		
Knot ID	x ($''$)	y ($''$)	μ_x ($''$ yr^{-1})	μ_y ($''$ yr^{-1})	μ_{tot} ($''$ yr^{-1})	μ_x ($''$ yr^{-1})	μ_y ($''$ yr^{-1})	μ_{tot} ($''$ yr^{-1})
S0	3.5	−16.7	−0.007	−0.011	0.013±0.005	...	...	...
S1	4.7	−18.0	−0.006	−0.013	0.014±0.004	0.00	0.00	0.00 ± 0.07
S2	6.2	−21.5	−0.006	−0.017	0.018±0.005	+0.05	−0.05	0.07 ± 0.07
S3	11.9	−27.3	+0.004	−0.021	0.021±0.008	0.00	−0.10	0.10 ± 0.07
S4	13.8	−38.1	+0.003	−0.036	0.036±0.007	0.00	−0.10	0.10 ± 0.07

[a]Positions relative to Star 16 of Wyckoff & Murray (1977).

Table 3

[Ar III] Knot Velocities and Directions

Knot ID	Δx, Δy μ^a ($''$ yr^{-1})	This Paper μ ($''$ yr^{-1})	V_t^b (km/s)	V_r^c (km/s)	V_{space} (km/s)	PA (deg)	Predicted μ Position Angles COE[d] (deg)	COE[e] (deg)	Pulsar (deg)
S0	0.011	0.013±0.005	120	···	···	215 ±16	206	214	152
S1	0.012	0.014±0.004	130	420	440	206 ±13	197	205	151
S2	0.015	0.018±0.005	170	720	740	198 ±10	187	194	152
S3	0.022	0.021±0.008	200	630	660	169 ±17	167	173	147
S4	0.035	0.036±0.007	340	400	525	175 ±11	168	172	153

[a]Proper motion values based on epoch 1995.0 knot displacements (Δx, Δy) from Trimble's center of expansion and assuming an expansion date of A.D. 1130.

[b]Average transverse velocity estimates based on our proper motion measurements and a 2 kpc distance.

[c]Radial velocities from MacAlpine et al. (1994).

[d]Measured from Trimble's (1968) center of expansion (COE).

[e]Measured from Nugent's (1998) center of expansion (COE).

REFERENCES

Blair, W. P., Davidson, K., Fesen, R. A., Uomoto, A., MacAlpine, G. M., & Henry, R. B. C. 1997, ApJS, 109, 473

Davidson, K., & Fesen, R. A. 1985, ARA&A, 23, 119

Fesen, R. A., Martin, C. L., & Shull, J. M. 1992, ApJ, 399, 599

Hester, J. J. et al. 1996, ApJ, 456, 225

Lawrence, S. S., & MacAlpine, G. M. 1994, BAAS, 26, 951

Lawrence, S. S., MacAlpine, G. M., Uomoto, A., Woodgate, B. E., Brown, L. W., Oliversen, R. J., Lowenthal, J. D., & Liu, C. 1995, AJ, 109, 2635

Kafatos, M. C., & Henry, R. B. C. 1985, "The Crab Nebula and Related Supernova Remnants - An Overview", (Cambridge, Cambridge Univ. Press)

MacAlpine, G. M., McGaugh, S. S., Mazzarella, J. M., & Uomoto, A. 1989, ApJ, 342, 364

MacAlpine, G. M., Lawrence, S. S., & Brown, B. A. 1993, BAAS, 25, 785

MacAlpine, G. M., Lawrence, S. S., Uomoto, A., Woodgate, B. E., Brown, L. W., Oliversen, R. J., Lowenthal, J. D., & Liu, C. 1992, BAAS, 24, 791

MacAlpine, G. M., Lawrence, S. S., Brown, B. A., Uomoto, A., Woodgate, B. E., Brown, L. W., Oliversen, R. J., Lowenthal, J. D., & Liu, C. 1994, ApJ, 432, L131

Michel, F. C., Scowen, P. A., Dufour, R. J., & Hester, J. J. 1991, ApJ, 368, 463

Nugent, R. L. 1998, PASP, 110, 831

Trimble, V. 1968, AJ, 73, 535

Trimble, V. 1985, in "The Crab Nebula and Related Supernova Remnants - An Overview", (Cambridge, Cambridge Univ. Press), p 257

Sankrit, R. et al. 1998, ApJ, 504, 344

Uomoto, A., & MacAlpine, G. M. 1987, ApJ, 160 L27

van den Bergh, S. 1970, ApJ, 160, L27

Wyckoff, S., & Murray, C. A. 1977, MNRAS, 180, 717

AAS LaTeX macros v5.0.

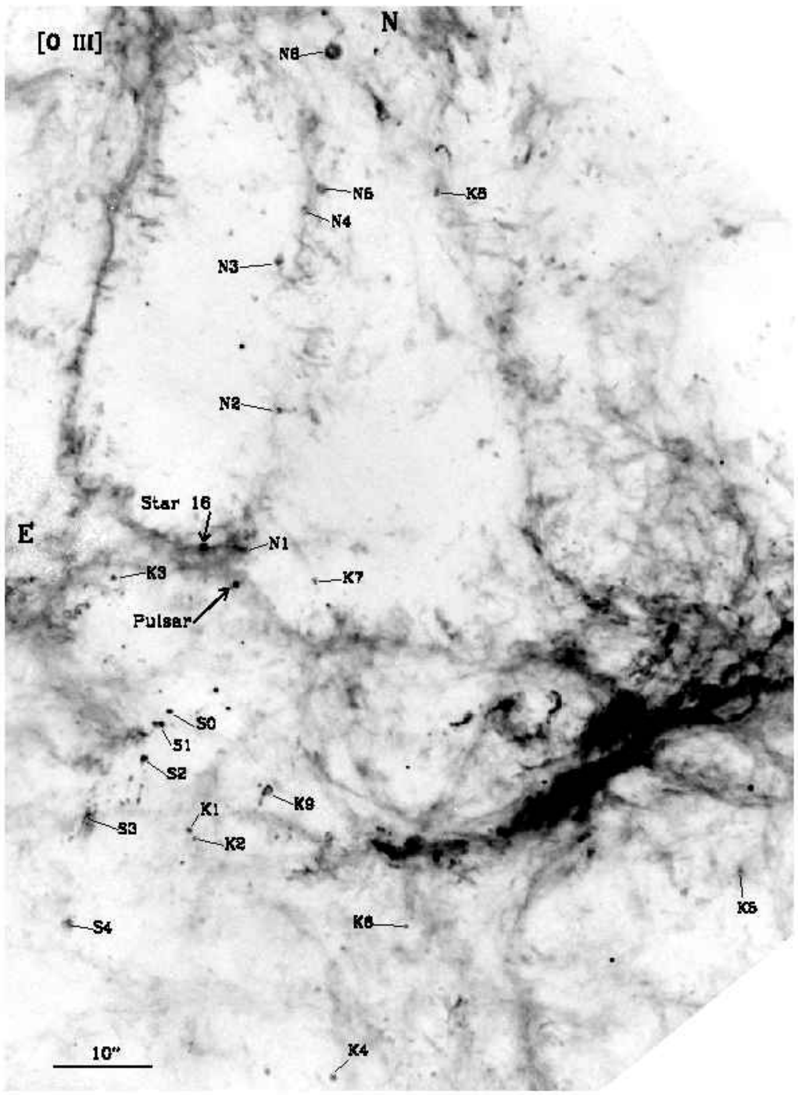

Fig. 1.— 1995 *HST* [O III] λ5007 WFPC2 image of the west-central region of the Crab Nebula showing the line of [Ar III] emitting knots (N1-N6 and S1-S4) described by MacAlpine et al. (1994). The field of view shown is approximately $1.3' \times 1.8'$. Other nebular knots having similar "semi-stellar" [O III] morphologies are shown in the image and labeled K1 – K9.

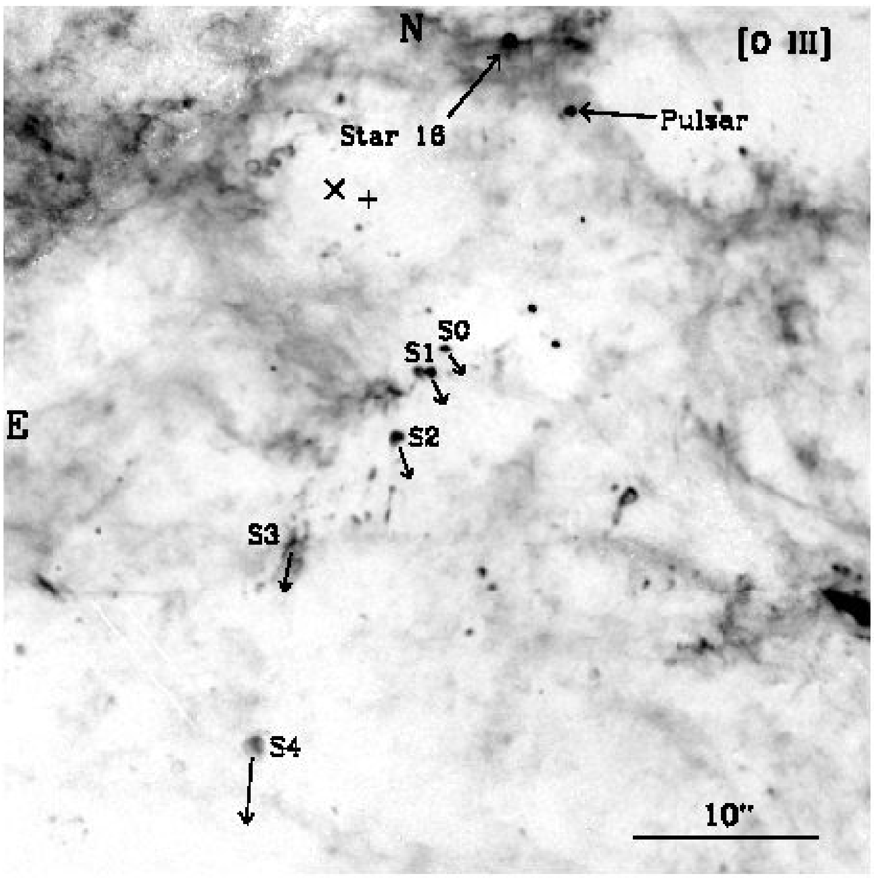

Fig. 2.— 1995 *HST* [O III] λ5007 WFPC2 image of the center of the Crab Nebula showing the directions of motion of the five southern knots. The length of the arrows corresponds to the distance that would be traveled in 100 years at the present velocity. The cross marks the position of the Trimble (1968) center of expansion, the x the position of the Nugent (1998) center of expansion.

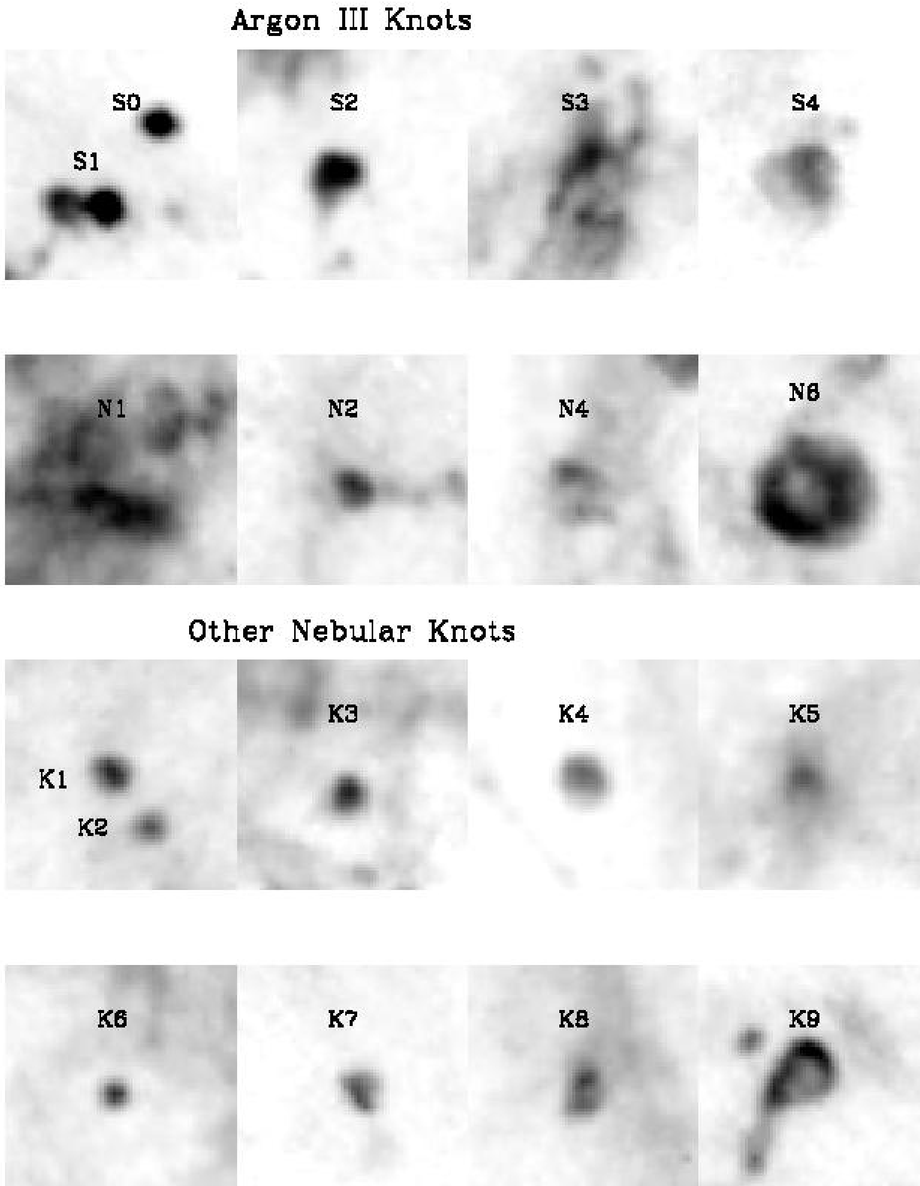

Fig. 3.— 1995 *HST* [O III] λ5007 WFPC-2 magnified ($0''.05$/pixel) images of bright [Ar III] emitting knots and of other nebular knots. Each box is $5''$ square.